

Infrared lines as probes of solar magnetic features

XI. Structure of a sunspot umbra with a light bridge

I. Rüedi¹, S.K. Solanki¹, and W. Livingston²

¹ Institute of Astronomy, ETH–Zentrum, CH–8092 Zürich, Switzerland

² National Solar Observatory, NOAO*, P.O. Box 26732, Tucson, AZ 85726, USA

Received 8 December 1994 / Accepted 17 March 1995

Abstract. We investigate the magnetic structure of an umbra and the light bridge it contains using spectra at $1.56\ \mu\text{m}$. The magnetic field strength in the umbra reaches over 3500 G on the first day of observation and 3200 G on the second and third days, while the field strength in the light bridge is reduced by 1000–1400 G relative to the nearby umbra. The magnetic vector is also found to be much more horizontal in the light bridge. There is evidence that the boundary between the strong and weak magnetic field is less than $1''$ wide, implying the presence of large currents there. At some locations a downflow of up to $1.5\ \text{km s}^{-1}$ is seen in the light bridge relative to the umbral material. Finally, we discuss the blending of the $1.5648\ \mu\text{m}$ line in sunspots and develop the depth of the OH $15650.7\ \text{\AA}$ line as a diagnostic of umbral temperatures.

Key words: Sun: magnetic fields – Sun: infrared – sunspots

1. Introduction

Sunspots often show a complex structure in the course of their evolution. The ideal picture of a circular umbra is seldom valid. Rather, umbrae often have intrusions of bright, penumbra-like material, which sometimes split an umbra into two parts, forming a light bridge. The structure and physical properties of these have so far been insufficiently studied. Their morphological appearance is commonly divided into three classes consisting of “photospheric”, “penumbral” and “umbral” light bridges (Bray & Loughhead 1964; Muller 1979; Sobotka et al. 1994). The members of the first group appear to be formed of normal photospheric material showing the typical granular structure of the photosphere, while the others consist of penumbral filaments extending into the umbra and made of individual grains (Muller 1979). Penumbral light bridges differ from umbral light bridges

by being brighter and wider. Only few spectroscopic observations of light bridges exist, so that their magnetic structure is poorly known. Beckers & Schröter (1969) found that the field was 200–300 G lower and over 5° more strongly inclined towards the horizontal, while Abdusamatov (1970) determined a much larger decrease of the magnetic field strength in a photospheric light bridge (from magnetographic observations). A field strength reduction of 800 G was found by Kneer (1973) in a partial light bridge. Finally, Lites et al. (1991) determined an upper limit to the magnetic field strength of approximately 1 kG in a photospheric light bridge. Rüedi et al. (1995, Paper X of the present series) carried out observations of chromospheric and photospheric magnetic flux over a broad stable light bridge and found $B = 1500\ \text{G}$ at both heights, although with low accuracy. Their smaller vertical field-strength gradient in the light bridge agrees with the results of Abdusamatov (1970). In this work, we analyse spectroscopic $1.56\ \mu\text{m}$ data of an isolated sunspot containing a penumbral light bridge. Due to the high Zeeman sensitivity of the observed $g = 3$ line we can reliably measure also the weaker field in the light bridge. The data and the general behavior of the observed region is briefly described in Sect. 2. Section 3 reviews the method used for the analysis. The results are summarized in Sect. 4 and discussed in Sect. 5.

2. Observations

A large sunspot ($60'' \times 90''$) was observed on 1st–3rd October 1993 with the McMath–Pierce telescope and the main spectrograph with the new infrared grating. Stokes $I \pm V$ were recorded consecutively at each wavelength on the 2nd and 3rd day of observation, while on the 1st day only Stokes I was recorded. The observed wavelength range contains the two Fe I lines at $15648.5\ \text{\AA}$ ($g = 3$) and $15652.9\ \text{\AA}$ ($g_{\text{eff}} = 1.53$). At each spatial position 3 or 4 wavelength scans (depending on the day of observation) were co-added in order to reduce distortions due to seeing. The high frequency noise of the highly oversampled data was reduced by Fourier filtering. For more information on the observational procedure we refer to Livingston (1991) and Solanki et al. (1992a, Paper II of the present series).

Send offprint requests to: I. Rüedi

* Operated by the Association of Universities for Research in Astronomy, Inc. (AURA) under cooperative agreement with the National Science Foundation.

Each day the sunspot was scanned along its major axis. The scan crossed the light bridge. White-light images of the spot are shown in Figs. 1a (1st October, referred to as day 1) and b (2nd October, referred to as day 2), in which the features cited below can be recognized. The observations were carried out from left (west) to right (east) along the horizontal white lines. The actual scans were considerably longer, but we only discuss the spectra in the marked portions. On 1st October, 1993, the first day of observations, the spot was located at $\mu = \cos \theta = 0.93$ and evolved rapidly. As can be seen in Fig. 1a the feature that evolved into the light bridge looked like a hook-shaped plume and extended only up to the middle of the umbra.¹ Other similar features of smaller size were present at the eastern umbra-penumbra boundary, but, with one exception were not observed spectroscopically. By 2nd October the spot already consisted of two main umbrae of the same polarity separated by a penumbral light bridge. Later in the day, this light bridge shrank slightly again and no longer completely divided the umbra. The position of this feature is located somewhat more westward than the hook-shaped light bridge of 1st October. At the eastern penumbral boundary the “plumes” seen on 1st October have grown into a light bridge which separates a small umbra from the main umbra. The spot did not evolve much between 2nd and 3rd October.

Here we concentrate on the data of 1st and 2nd October which gave the most interesting results. The data of the 3rd October (day 3) were also analysed in the same manner as the data discussed here, but did not provide any new insights.

3. Data analysis

The data were fit using the inversion code described by Solanki et al. (1992b, 1994, Papers V and VII of the present series) and by Emonet (1992). Stokes I and (when present) V profiles were calculated in LTE through a two-component model atmosphere composed of a magnetic and a non-magnetic part. The synthetic profiles were then compared with the data and the free parameters of the model were varied until a minimum in χ^2 was achieved. For the non-magnetic component we used the quiet sun model of Maltby et al. (1986), extended downward into the convection zone following Spruit (1977), while the magnetic component was produced by interpolating $T(\tau)$ between the umbral models of Maltby et al. (1986) and the HSRA (quiet-sun model of Gingerich et al. 1971) to obtain the desired temperature². During the fitting procedure, the temperature was kept fixed and was determined from the continuum intensity of the corresponding spectrum. The conversion between continuum intensity and $T(\tau_{1.56} = 1)$ was made by calculating the former on a fine grid of models with different temperatures and

¹ Its similarity to a dinosaur (or more precisely a brontosaurus) led us to call this sunspot the ‘Jurassic’ spot.

² The HSRA gave better results than, say, the quiet-sun model of Maltby et al. (1986)

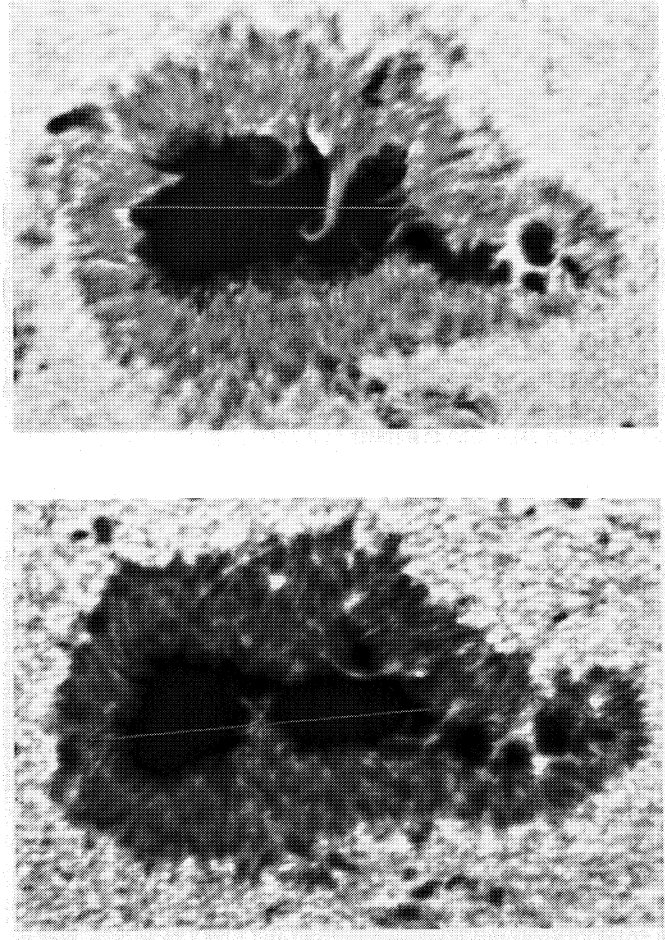


Fig. 1. White-light picture of the Jurassic spot on 1st October (top panel) and 2nd October (bottom panel). West is to the left, north is in the downward direction

interpolating. The conversion factor was calibrated using quiet sun spectra³.

Where the $g_{\text{eff}} = 1.53$ line was sufficiently free of OH blends, i.e. when the temperature was high enough, both lines were fitted simultaneously with the same physical parameters. Otherwise, the $g = 3$ line was fitted on its own.

The relevant free parameters of the inversion were the height independent magnetic field strength B , the inclination angle γ between the magnetic field vector and the line of sight, a macroturbulent velocity broadening v_{mac} and the filling factor α , which was set to 1.0 when Stokes I was fitted alone. This seemed to be a good approximation, since the filling factor did not deviate much from 1.0 for the fits to the data of 2nd October when both Stokes I and V were present. Furthermore, due to better seeing conditions the stray-light present in the 1st October data is expected to be lower than on 2nd October.

³ Fits to the line profiles with temperature as a free parameter give similar results, except that the derived temperature scatters around the value derived from the continuum intensity

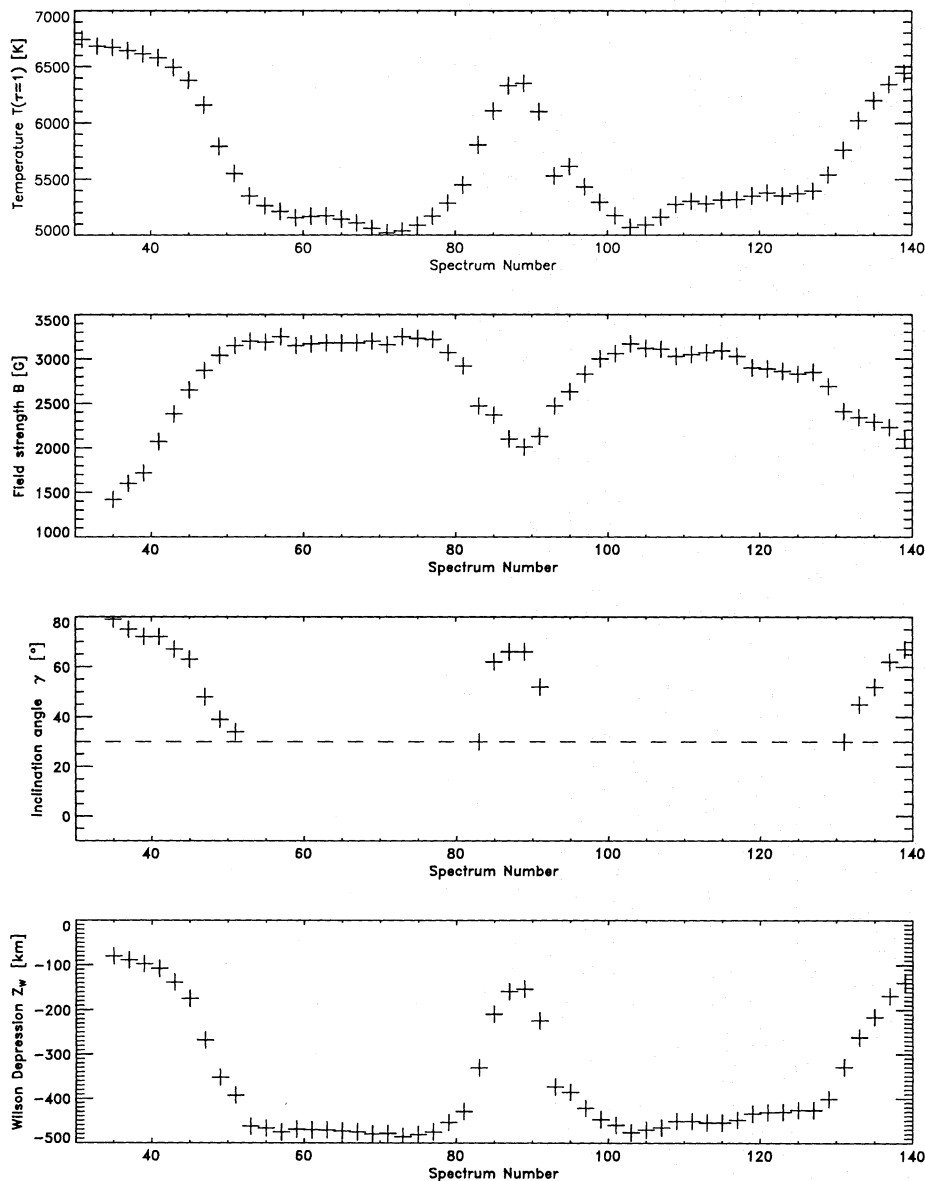


Fig. 2. Various atmospheric parameters along the W-E scan shown on Fig. 1b, i.e. on 2nd October. **Top panel:** Temperature. **2nd panel:** Magnetic field strength B . **3rd panel:** Inclination angle γ between magnetic vector and line of sight. **Bottom panel:** Wilson depression Z_W

4. Results

Figure 2 shows the results obtained from the inversion of the 2nd October data when Stokes I and V were available. The points from left to right correspond to the east to west scan through the spot, shown in Fig. 1b. Only a part of the total scan is shown in Fig. 2, since the Stokes V profiles from the outer penumbra, where the magnetic field is practically perpendicular to the line-of-sight, are considerably distorted by instrumental cross-talk. Neighboring points are separated by $1.2''$. The results obtained from the data on the other days are similar, except for a few profiles on 1st October, when the spot evolved quickly and the seeing was better. Those peculiar profiles (light bridge, penumbra) will be treated separately in Sects. 4.4 and 4.6.

The top panel of Fig. 2 shows the temperature obtained from the continuum intensity as explained in Sect. 3. The plotted range contains the light bridge in the middle (warm feature), surrounded on both sides by the cool umbra, with the inner part

of the penumbra visible on both ends of the plot. The second panel shows the magnetic field strength B as obtained from the inversion, while the third panel represents the inclination angle γ between the magnetic field vector and the line of sight. The bottom panel shows the Wilson depression Z_W determined according to the technique described in Sect. 4.3.

On day 2, every profile could be fitted using only one magnetic component. In the following we discuss each parameter separately.

4.1. Magnetic field strength B

This large spot exhibits a strong magnetic field, which reaches 3250 G on day 2 (Fig. 2). On the previous day the maximum observed field strength was even larger and reached 3560 G (Fig. 3). This is close to the maximum field strengths seen by Kopp & Rabin (1992) or found in Paper II, which were ≈ 3500 G, and may give an indication that there is an upper

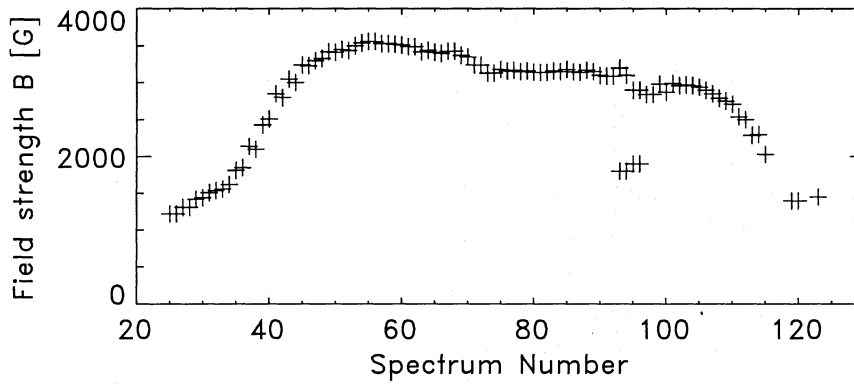


Fig. 3. Magnetic field strength B along the W-E scan shown on Fig. 1a, i.e. on 1st October

limit to the field strength in umbrae of simple sunspots, except, perhaps, on short timescales. In the light bridge the magnetic field strength is strongly reduced. It achieves values similar to those observed in the mid penumbra. This is still ≈ 1000 G larger than the values found in Lites et al. (1991).

On the west side of the spot (left of Fig. 2), the penumbra is narrower than on the east side and B varies almost as rapidly as at the umbra–light bridge boundary. The boundary of the light bridge is considerably sharper than we are able to resolve directly. This is suggested by fits to the peculiar profiles discussed in Sect. 4.4.

4.2. Inclination angle γ

The inclination angle between the magnetic vector and the line of sight is plotted in the third panel of Fig. 2. The magnetic field has the same polarity at all the plotted positions. Since only sufficiently large γ can be diagnosed from Stokes I and V (Paper V), only $\gamma > 30^\circ$ have been plotted in Fig. 2. At the transition between the umbra and the light bridge the inclination angle changes very rapidly over a distance of a few arc s (the distance between two sample points is $\approx 1.2''$). This variation is faster than in both penumbrae, in contrast to the variation of the magnetic field strength, which is similar at the light bridge boundary to that of the narrower, eastern penumbra. We believe this variation of the inclination angle is real and not due to stray-light, since in the light bridge we expect less stray-light from the quiet sun and the penumbra, which could be mistaken for too large an inclination angle, than in the umbra. Zirin & Wang (1993) have also shown examples of large horizontal gradients of the magnetic inclination, although their results refer to complex sunspots containing both magnetic polarities, (δ spots).

4.3. Wilson depression Z_W

Finally, the Wilson depression Z_W (bottom panel of Fig. 2) was determined with the method used by Solanki et al. (1993, Paper VI of the present series; cf. Martínez Pillet & Vázquez 1993) under the assumptions spelled out by Maltby (1977). Z_W is defined in Eq. (1) as being the difference between the height

of $\tau = 1$ at 5000 \AA in the quiet sun and that of $\tau = 1$ at the considered wavelength inside the spot,

$$\begin{aligned} Z_W(r, \lambda) &= z(\tau_{0.5} = 1, r > r_p) - z(\tau_\lambda = 1, r) \\ &= -z(\tau_\lambda = 1, r). \end{aligned} \quad (1)$$

Here z is the height above the layer of continuum formation at 5000 \AA , r the radial distance from spot center, r_p the penumbral radius, τ the continuum optical depth and λ the wavelength of the observations.

In order to determine the Wilson depression the integrated form of the radial component of the magnetohydrostatic force balance equation in cylindrical coordinates is used (e.g. Maltby 1977).

$$\begin{aligned} P_0(z) - P(r, z) &= \\ &= \frac{1}{8\pi} \left(B_z^2(r, z) + 2 \int_r^a B_z(r', z) \frac{\partial B_r(r', z)}{\partial z} dr' \right) \\ &= B_z^2(r, z)/8\pi + F_c(r, z)/8\pi \end{aligned} \quad (2)$$

In this equation, the indices r and z denote the radial and vertical coordinates respectively, B the magnetic field strength and P the gas pressure. P_0 refers to the pressure in the quiet sun model and the point a lies outside the spot in the quiet sun. The second term on the right hand side has been abbreviated as F_c and represents the integrated magnetic curvature.

Following Solanki et al. (1993) we neglect the curvature term F_c . For a positive F_c the true Z_W should be larger than the value obtained from Eq. (2). The uncertainty in γ , which is largest in the umbra, only has a small effect on the value of Z_W .

The maximum Wilson depression seen in Fig. 2 is 480 km. This value corresponds to the largest value obtained by Solanki et al. (1993). The magnetic field strength related to these two points is also similar: 3200 G. On the previous day, when the magnetic field strength was larger, reaching over 3500 G, the corresponding Wilson depression was also enhanced by about 30 km, but in the light bridge it remained at 150 km. Note that Z_W on day 1 is less accurate than on day 2, due to the absence of Stokes V observations.

Finally, the relationship between temperature and magnetic field is illustrated in Fig. 4 for the whole data set. There are two points to note. Firstly, the magnetic structure evolved considerably over the three days. Not only was the umbral field strength reduced on the 2nd and 3rd days, but B at the umbral–penumbral boundary was also smaller, particularly on one side

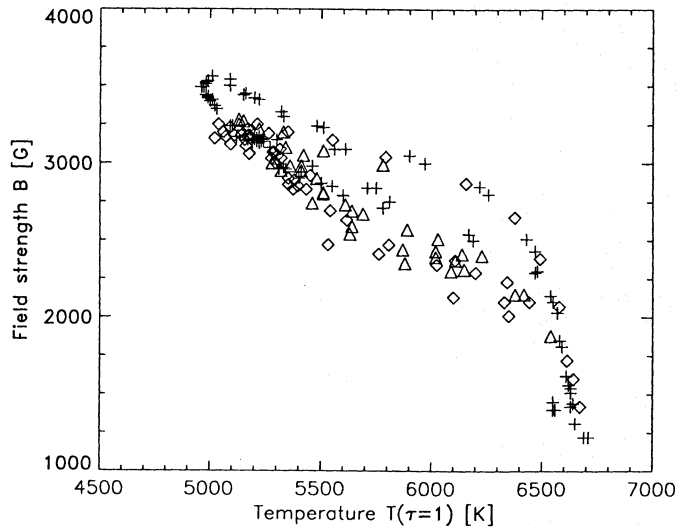


Fig. 4. Magnetic field strength as a function of temperature for the whole data set. The crosses correspond to 1st October data, the diamonds to 2nd October and the triangles to 3rd October

of the spot. On the whole, the change in B appears to have been larger than the corresponding changes in T , suggesting that it was not primarily a warming of the sunspot which caused these effects. A change in the magnetic curvature forces due to the rapid rearrangement of the field is a likely candidate. Secondly, the presence of considerable curvature forces in some parts of the sunspot or an inhomogeneous Z_W surface is suggested by the two quite distinct branches between $T=5500$ K and 6500 K in Fig. 4.

4.4. Peculiar light-bridge profiles

On day 1, the light-bridge spectra showed much broader σ -components than on the second day and some of them, in addition, were asymmetric. It was impossible to fit these spectra with only one magnetic component, but all of them could be acceptably reproduced when two magnetic components were combined. The fact that two distinct σ -peaks are seen indicates that the boundary between the low and high field regions is considerably thinner than our spatial resolution element. We estimate that the boundary is sharper than 1 arc s.

Figure 5 shows one of the asymmetric light-bridge profiles recorded on 1st October (solid curve). Note the double-peaked shape of the blue σ -component. It implies that two distinct magnetic components were present in the resolution element, while the asymmetry of the profile suggests a velocity shift between them. The dashed line is the fit obtained using two magnetic components. The first component was assumed to correspond to the surrounding umbra, i.e. a strong magnetic field (3200 G) inclined by 40° to the line of sight. The second component required a much lower field strength of 1800 G and had a larger inclination angle of 60° . Due to the asymmetry of the line profile, the two components had to be shifted against each other in order to reproduce the observed profile acceptably. The weak-field component is red-shifted by 1.1 km s^{-1} relative to the

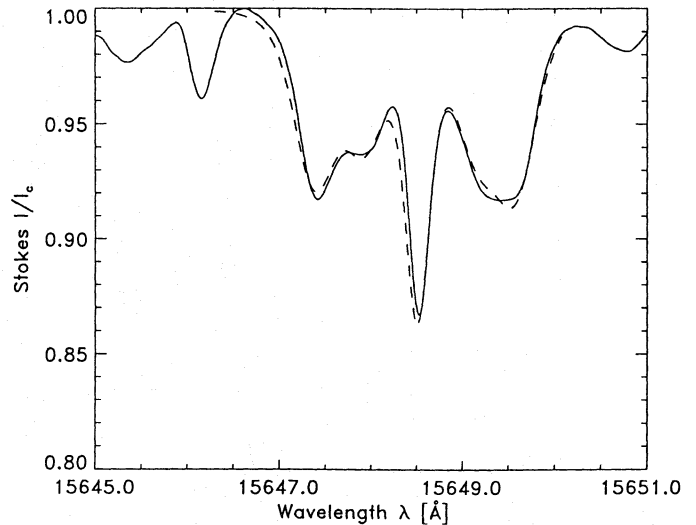


Fig. 5. Stokes I line profile of Fe I 15648.5 Å observed in the light bridge on 1st October (solid curve) and fit (dashed curve) using a model composed of two magnetic components

strong-field component. The final synthetic profile (dashed) is a compound of 45 and 55% of weak and strong field, respectively, if they both have the same continuum intensity. Taking the different continuum intensity into account we get approximately 30% weak-field and 70% strong-field material in the resolution element.

All four light-bridge profiles of 1st October required a combination of this kind to fit the data acceptably. The field strength of the strong component varied between 2900 and 3200 G, while that of the weak components amounted to 1800 – 1900 G. The inclination angle was 40° and $60 - 70^\circ$ and the contribution 65 – 70% and 30 – 35% for the strong and weak component, respectively.

In two out of four cases a shift between the two components was present. The weak-field was red-shifted against the strong-field and the maximum shift observed was 1.5 km s^{-1} . There is little sense in attempting to improve the fit further due to the blend discussed in Sect. 4.5.

4.5. Blends

Due to an iron blend at 15647.4 Å the Stokes I profile of the $g = 3$ line is asymmetric for field strength values larger than approximately 1500 G. In Fig. 6 three Stokes I profiles of the $g = 3$ line are plotted in the order of increasing field strength. The inversion of these spectra together with their Stokes V counterparts yielded the following field strengths values: 1600 G, 2380 G and 3040 G for the left, middle and right panel, respectively. In the first panel, where the line is least split, the blend at 15647.4 Å is seen as a shoulder on the blue σ -component of the $g = 3$ line. For increasing field strengths it overlaps increasingly with the blue σ -component of Fe I 15648 Å which lies exactly on the blend at $B = 3200$ G. Thus the asymmetry also increases with field strength for $B \lesssim 3200$ G. A weaker blend is present on the red side of the line. It lies closer to the loca-

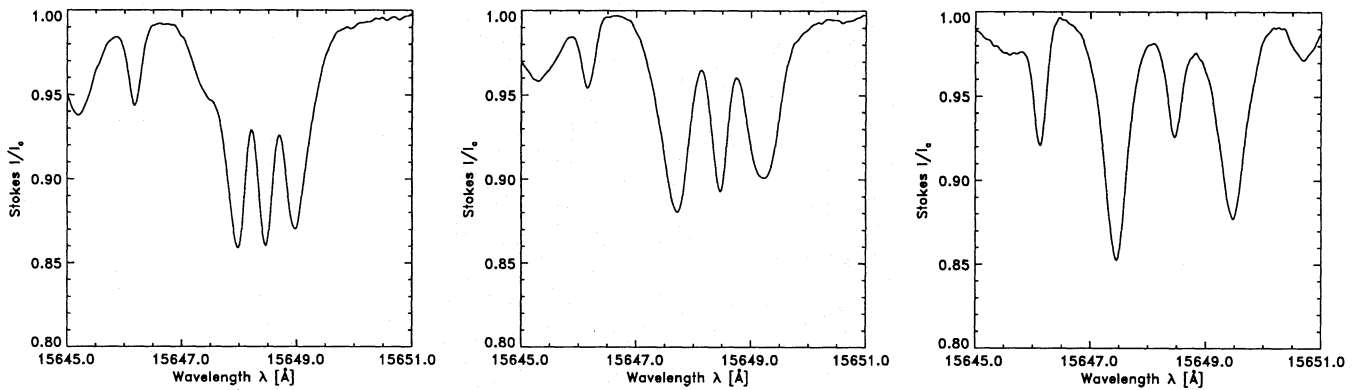


Fig. 6. Stokes I profiles of the $g = 3$ line at 15648.5 \AA . From left to right the field strength corresponding to these spectra are 1600 G, 2380 G and 3040 G

tion of the π -component and is partly responsible for the width of the 1.5648 \mu m line's red σ -component. Since these blends appear to be only slightly Zeeman sensitive, they have a much smaller effect on the Stokes V profile. On the other hand, we expect that for a smaller filling factor or more stray light (e.g. in pores) the effects of the blends on Stokes I are larger due to the relative weakness of the σ -components in this case. These blends can then falsify results if only Stokes I is available, e.g. on cool stars (Valenti et al. 1995), or more immediately, in our data of 1st October. Only asymmetries that go beyond the 'normal' value (illustrated in Fig. 6 for a high filling factor) should be interpreted in terms of velocity gradients, etc. This limits the accuracy of the results obtained from the asymmetric profiles discussed in Sect. 4.4 and 4.6.

4.6. Asymmetric penumbral profiles

A penumbral profile observed on 1st October, when the spot evolved rapidly, is shown in Fig. 7 (solid line). It possesses a deeper red σ -component unlike other penumbral profiles (cf. Fig. 6), although they span the temperature, magnetic field strength and inclination range containing the parameters of this profile. Thus, it appears highly unlikely that an extremely temperature-sensitive blend or instrumental cross-talk is responsible for this asymmetry.⁴

This feature must therefore be of solar origin and is restricted to a small area. A reasonable fit to this profile has been obtained using two magnetic components having a field strength difference of 500 G (dashed curve in Fig. 7). The weaker component is shifted in wavelength relative to the strong component by an amount corresponding to 3.5 km s^{-1} along the line of sight (this line shift must be due mainly to a vertical velocity, since due to the small θ value it would amount to a horizontal velocity of 9.5 km s^{-1} , which would be in excess of the local sound speed). It is interesting to note that on the 1st October picture

⁴ In order to produce an asymmetry of the observed magnitude, the cross-talk would anyhow have to be much larger than that expected from the Muller-matrix of the telescope at the time of these observations.

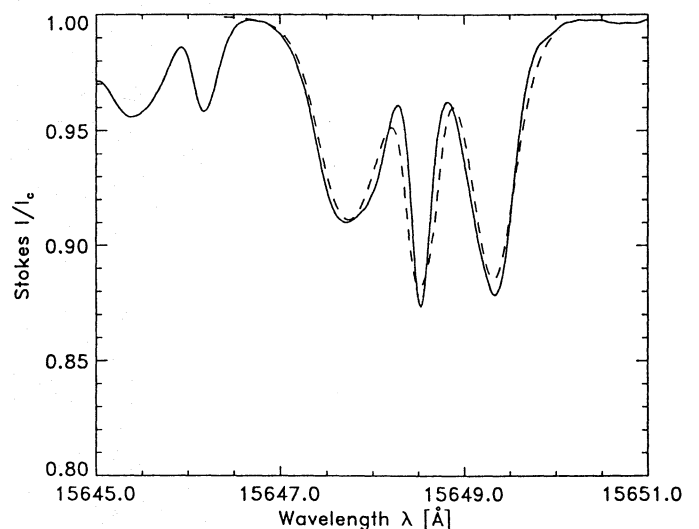


Fig. 7. Observed asymmetric Stokes I profile (solid curve) and synthetic profile (dashed curve) composed of two magnetic components of different field strength and shifted relative to each other by an amount corresponding to 3.5 km s^{-1} along the line of sight

of the spot, plumes of the same kind as the light bridge, but smaller in extent, can be seen at and near the location at which this profile was recorded. The spot evolved particularly strongly around this location, so that on the next day a light bridge had completely crossed the umbra at this position, leaving a small umbra on one side separated from the two main umbrae on the other side. These quick changes are consistent with the high relative velocities obtained from the fits.

4.7. Line shifts

For those profiles which could be satisfactorily reproduced with only one magnetic component we determined the wavelength difference between the central position of the synthetic profile and a reference wavelength. This gives information on the line of sight component of matter flows. In the umbra, where blends significantly distort the Stokes I profile, the obtained values are not reliable.

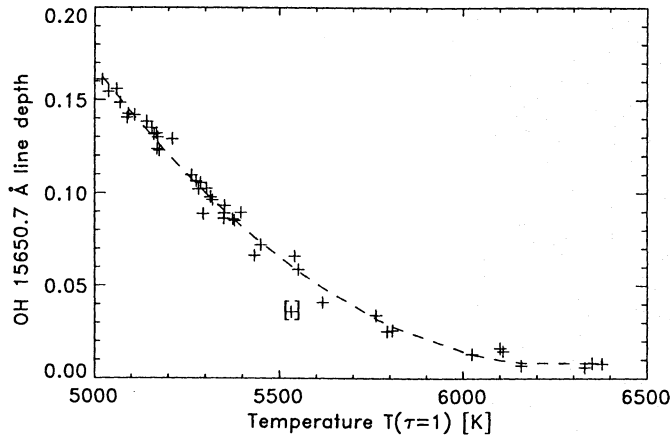


Fig. 8. Depth of OH 15650.7 Å line in units of the continuum intensity, as a function of the temperature at the height of formation of the continuum, $T(\tau_{1.6} = 1)$

The light bridge spectra did not show any systematic flow relative to the penumbral spectra. This means that on the 2nd day no coherent flow with a component along the line of sight in the light bridge existed, unlike on 1st October where the light-bridge profiles required two magnetic components shifted by 1.5 km s^{-1} relative to each other in order to be reproduced properly.

4.8. OH line at 15650.7 Å: a temperature diagnostic

At 15650.7 Å, between the two observed Fe I lines, lies an OH line which only becomes prominent in the umbra. The temperature dependence of its depth relative to the continuum is shown in Fig. 8.

Between 5000 and 5600 K, the scatter present in the plot is small. The line depth increases monotonically as the temperature decreases. In this temperature range, due to the numerous lines blending the $g_{\text{eff}} = 1.53$ line and to the poor temperature sensitivity of the $g = 3$ line the temperature determination is problematic if the continuum intensity is poorly known (stray light) or if no quiet-sun intensity reference is available. The advantage of the OH line is that it provides a temperature diagnostic independent of other observations.

Note that the lowest point at 5530 K (in square brackets) corresponds to spectrum number 93, which has a very low continuum intensity and was consequently assigned a low temperature, as seen in Fig. 2. This is probably an artifact of the measurement and should not be considered as intrinsic scatter of the data. The solid curve is a least square fit to the data points, excluding spectrum No. 93. The curve satisfies the relation: $4.0112 - 1.2808 \cdot 10^{-3} T + 1.0244 \cdot 10^{-7} T^2$. Together with the CN line at $1.56462 \mu\text{m}$, which is mainly sensitive to intermediate, i.e. penumbral, temperatures, the OH line covers the whole run of sunspot temperature.

5. Discussion and conclusions

We have observed and analysed $1.56 \mu\text{m}$ spectra of the umbra of a large, complex sunspot on three successive days. The outline of the whole sunspot and in particular of the bright structures in the umbra changed considerably on the first day, but less on the second and third day. Of particular interest have been protrusions of the penumbra into the umbra and a light bridge. The magnetic structure of the umbra and penumbra are quite normal. In the dark part of the umbra we find a strong field ($B \approx 2900 - 3600 \text{ G}$ for $T(\tau_{1.6} = 1) \lesssim 5500 \text{ K}$ on day 1, and $2800 - 3200 \text{ G}$ on days 2 and 3), which is inclined by less than 40° . The continuum $\tau = 1$ level is also depressed by 400–500 km (Wilson depression) in the absence of curvature forces. In the penumbra the field strength is found to gradually decrease outwards, coupled with a corresponding increase of the inclination to the vertical. Bright protrusions of penumbra-like material into the umbra show properties typical of the mid-penumbra, i.e. a field strength 1000–1500 G lower than in the nearby umbra and a $20 - 30^\circ$ larger inclination to the vertical. The intrusions and light bridge also have a temperature, a temperature-field strength correlation and consequently a Wilson depression typical of the penumbra.

The depressed field strength in the light bridge is in qualitative agreement with previous investigations (Beckers & Schröter 1969; Abdusamatov 1970; Kneer 1973; Lites et al. 1991), although the actual values scatter considerably. A part of this scatter probably stems from the different Zeeman sensitivities and heights of formation of the spectral lines used by the different investigators, but given that different light bridges have different brightnesses, a part of this scatter may well be solar. The larger inclination to the vertical also agrees with Beckers & Schröter qualitative findings.

One major difference between the light-bridge and normal penumbra is the extremely large field strength gradient at the light-bridge boundary, $\lesssim 1400 \text{ G/arc s}$ (recall that the normal umbra to penumbra transition is smooth in B). Such a large gradient also implies an extremely large current density. Assuming other gradients to be small we obtain a current density of at least 0.16 A m^{-2} , which is over 20 times larger than the largest current seen by Lites & Skumanich (1990) in a large symmetric sunspot and only a factor of 3 lower than the maximum value found in complex sunspots containing both magnetic polarities by Zirin & Wang (1993). Although there is no evidence for any systematic flow of the light-bridge material on day 2 and 3, a distinct redshift is seen relative to the nearby umbra on the first day. In particular, on the first day, when the seeing was best, the transition between umbra and light bridge was abrupt, within $1-2''$.

How are these observations to be interpreted? Could differences in magnetic properties between light bridge and umbra simply be a result of the different depth in the atmosphere to which one sees in these two features? Our analysis suggests that the difference in heights is roughly 300–500 km. The resulting gradients are much too large, e.g. $dB/dz \approx 4.2 \text{ G km}^{-1}$, which is larger than generally observed, and $d\gamma/dz \approx 7^\circ/100 \text{ km}$,

which is 7 times larger than the upper limit set in Paper VI (imposed by requiring that a static equilibrium must be maintained, under various assumptions). If we assume the presence of considerable curvature forces, so that $Z_W \approx 800$ km in the umbra instead of 400-500 km (800 km is the maximum value according to Gokhale & Zwaan 1972), then the resulting dB/dz lies within the bounds of observations (Wittmann 1974; Balthasar & Schmidt 1993; Paper VI; Bruls et al. 1995 Paper VIII of the present series). $d\gamma/dz \approx 4^\circ/100$ km, however, is still roughly a factor of 4 larger than the upper limit of Paper VI. Recall also that in Paper X we found some evidence for a smaller $d(B \cos \gamma)/dz$ in a light bridge than in the nearby umbra.

The more likely possibility is that the magnetic structure is truly different in the light bridge. Note that since the umbra on both sides of the light bridge has the same polarity, the magnetic field does not form a loop there, so that this cannot be the reason for the more horizontal field. We rather expect that the stronger umbral magnetic field pushes the weaker light-bridge field together, so that at a higher level, where gas pressure plays a minor role, they become almost equal in strength. Probably the light-bridge field also is azimuthally skewed, pointing towards the nearer penumbra, but only measurements of the full Stokes vector can decide this point.

In summary the penumbral protrusions and light bridge observed by us show properties typical of the penumbra, largely unmodified by the closeness of the umbra. In view of the fact that these structures are many photon mean-free paths across this may not be so surprising. Thus our results are compatible with the findings of Lites et al. (1993), who find a more vertical and stronger field in umbral protrusions into the penumbra, while we find a weaker, more horizontal field in the penumbral protrusions into the umbra. The large horizontal gradients in inclination we find at the edges of penumbral protrusions are in good agreement with the results of Zirin & Wang (1993). Rüedi et al. (1995) did not observe a lower field strength at photospheric heights in the light bridge they analysed. Their results, however, may be affected by the lower magnetic sensitivity of the line they used which consequently is also more susceptible to umbral stray-light than the $1.56 \mu\text{m}$ line.

Acknowledgements. We thank J. Harvey for providing us with his code for calculating the Muller matrix of the McMath-Pierce telescope.

References

- Abdusamatov K.I., 1970, *Soviet Astron. AJ* **14/1**, 64
 Balthasar H., Schmidt W., 1993, *A&A* **279**, 243
 Beckers J.M., Schröter E.H., 1969, *Sol. Phys.* **10**, 384
 Bray R.J., Loughhead R.E., 1964, *Sunspots*, Chapman and Hall
 Bruls J.H.M.J., Solanki S.K., Carlsson M., Rutten R.J., 1995, *A&A* **293**, 225 (Paper VIII)
 Emonet Th., 1992, *Diplomarbeit*, ETH, Zürich
 Gingerich O., Noyes R.W., Kalkofen W., Cuny Y., 1971, *Sol. Phys.* **18**, 347
 Gokhale M.H., Zwaan C., 1972, *Sol. Phys.* **26**, 52
 Kneer F., 1973, *Sol. Phys.* **28**, 361
 Kopp G., Rabin D., 1992, *Sol. Phys.* **141**, 253
 Lites B.W., Skumanich A., 1990, *ApJ* **348**, 747
 Lites B.W., Bida T.A., Johannesson A., Scharmer G.B., 1991, *ApJ* **373**, 683
 Lites B.W., Elmore D.F., Seagraves P., Skumanich A.P., 1993, *ApJ* **418**, 928
 Livingston W., 1991, in *Solar Polarimetry*, L. November (Ed.), National Solar Obs., Sunspot, NM, p. 356
 Maltby P., 1977, *Sol. Phys.* **55**, 335
 Maltby P., Avrett E.H., Carlsson M., Kjeldseth-Moe O., Kurucz R.L., Loeser R., 1986, *ApJ* **306**, 284
 Martínez Pillet V., Vázquez M., 1993, *A&A* **270**, 494
 Muller R., 1979, *Sol. Phys.* **61**, 297
 Rüedi I., Solanki S.K., Livingston W., 1995, *A&A* **293**, 252 (Paper X)
 Sobotka M., Bonet J.A., Vázquez M., 1994, *ApJ* **426**, 404
 Solanki S.K., Rüedi I., Livingston W., 1992a, *A&A* **263**, 312 (Paper II)
 Solanki S.K., Rüedi I., Livingston W., 1992b, *A&A* **263**, 339 (Paper V)
 Solanki S.K., Walther U., Livingston W., 1993, *A&A* **277**, 639 (Paper VI)
 Solanki S.K., Montavon C.A.P., Livingston W., 1994, *A&A* **283**, 221 (Paper VII)
 Spruit H.C., 1977, *Ph.D. Thesis*, Univ. Utrecht
 Valenti J.A., Marcy G.W., Basri G., 1995, *ApJ* **439**, 939
 Wittmann A.D., 1974, *Sol. Phys.* **36**, 29
 Zirin H., Wang H., 1993, *Nat.* **363**, 426

This article was processed by the author using Springer-Verlag \TeX A&A macro package 1992.